The EMBO Journal Vol. 19 No. 17 pp. 4589–4600, 2000

Scar/WAVE-1, a Wiskott–Aldrich syndrome protein, assembles an actin-associated multi-kinase scaffold

Ryan S.Westphal, Scott H.Soderling, Neal M.Alto[1], Lorene K.Langeberg and John D.Scott[2]

Howard Hughes Medical Institute, Vollum Institute and [1]Department of Cellular and Developmental Biology, The Oregon Health Sciences University, 3181 S.W. Sam Jackson Park Road, Portland, OR 97201-3098, USA

[2]Corresponding author
e-mail: scott@ohsu.edu

R.S.Westphal and S.H.Soderling contributed equally to this work

WAVE proteins are members of the Wiskott–Aldrich syndrome protein (WASP) family of scaffolding proteins that coordinate actin reorganization by coupling Rho-related small molecular weight GTPases to the mobilization of the Arp2/3 complex. We identified WAVE-1 in a screen for rat brain A kinase-anchoring proteins (AKAPs), which bind to the SH3 domain of the Abelson tyrosine kinase (Abl). Recombinant WAVE-1 interacts with cAMP-dependent protein kinase (PKA) and Abl kinases when expressed in HEK-293 cells, and both enzymes co-purify with endogenous WAVE from brain extracts. Mapping studies have defined binding sites for each kinase. Competition experiments suggest that the PKA–WAVE-1 interaction may be regulated by actin as the kinase binds to a site overlapping a verprolin homology region, which has been shown to interact with actin. Immunocytochemical analyses in Swiss 3T3 fibroblasts suggest that the WAVE-1 kinase scaffold is assembled dynamically as WAVE, PKA and Abl translocate to sites of actin reorganization in response to platelet-derived growth factor treatment. Thus, we propose a previously unrecognized function for WAVE-1 as an actin-associated scaffolding protein that recruits PKA and Abl.

Keywords: AKAP/anchoring protein/cytoskeleton/protein kinase targeting/signal transduction

Introduction

Understanding the sequence of signaling events that direct reorganization of the actin cytoskeleton is an important theme in the regulation of many cellular events (Hall, 1998). Thus, the spatial organization of signal transduction proteins at the cytoskeleton has become an area of intense interest. At the heart of this process is a molecular architecture maintained by scaffolding, anchoring and adaptor proteins (Pawson and Scott, 1997) that control the flow of signals emanating from transmembrane receptors to downstream effectors of the actin cytoskeleton (Hall, 1998). Principal targets are the Rho GTPases Rho, Rac and Cdc42, which promote distinct cytoskeletal changes leading to the formation of stress fibers, lamellipodia or filopodia, respectively (Hall, 1998; Higgs and Pollard, 1999). These distinct actin remodeling events are directed through association with the Wiskott–Aldrich syndrome protein (WASP) family of scaffolding proteins (Higgs and Pollard, 1999; Mullins, 2000). This family is named after its founding member, the Wiskott–Aldrich syndrome protein (WASP), which is mutated in a rare X-linked immunodeficiency disease (Snapper and Rosen, 1999). More recently, a ubiquitously expressed paralog, N-WASP, has been identified (Miki *et al*., 1996). Another WASP-related protein, Scar-1, was isolated originally in a genetic screen of *Dictyostelium discoideum* for proteins downstream of the chemotaxis receptor for cAMP, cAR2 (Bear *et al*., 1998). Subsequently, three mammalian Scar orthologs named WAVE-1, WAVE-2 and WAVE-3 have been cloned (Miki *et al*., 1998; Suetsugu *et al*., 1999). Each WASP family member functionally couples individual Rho GTPases to the Arp2/3 complex, a group of seven related proteins that function to nucleate actin polymerization and facilitate dendritic branching of actin filaments (Higgs and Pollard, 1999; Machesky *et al*., 1999; Blanchoin *et al*., 2000). These scaffolding proteins provide a molecular bridge that links Rho family members to the Arp2/3 complex. Thus, in response to signals from transmembrane receptors, WASP family members mediate the dynamic assembly of actin-based protein complexes at sites of actin remodeling.

Not surprisingly, these multifunctional proteins are composed of modular domains. For example, the N-terminal regions of WASP and N-WASP contain a CRIB domain that is responsible for direct interaction with Cdc42, whereas the three Scar/WAVE isoforms are believed to couple with Rac through an as yet undefined mechanism (Kim *et al*., 2000; Mullins, 2000). The central core of each WASP protein has several proline-rich sequences that interact with various SH3 proteins and the G actin-binding protein profilin (Miki *et al*., 1998; Mullins, 2000). Association with the actin cytoskeleton occurs through two conserved binding motifs: a verprolin homology (VPH) domain and a C-terminal acidic domain that binds to the Arp2/3 complex (Machesky *et al*., 1999).

Using a proteomics approach, we now demonstrate that the Abelson tyrosine kinase (Abl) and the cAMP-dependent protein kinase (PKA) are WAVE-1-binding partners inside cells. Thus, WAVE-1 can be classified as an A-kinase anchoring protein (AKAP), a growing family of cellular organizing proteins that tether PKA to defined subcellular sites via high affinity protein–protein interactions with the R subunit dimer of the PKA holoenzyme (Colledge and Scott, 1999). Immunocytochemical studies in Swiss 3T3 cells show that a pool of WAVE migrates from focal adhesions to sites of actin reorganization upon treatment with platelet-derived growth factor (PDGF).

These studies also demonstrate that both kinases move to these sites, suggesting that WAVE-1 may participate in the recruitment of kinases to sites of active cytoskeletal remodeling.

Results

Identification of WAVE-1 as an anchoring protein for PKA and Abl kinase

Although many modular adaptor proteins and AKAPs have been identified, few, if any of these anchoring proteins associate with serine/threonine and tyrosine kinases. Therefore, glutathione *S*-transferase (GST) fusion proteins encompassing the SH3 domains from three tyrosine kinases, Abl, Fgr and vSrc, and the SH3 domain of phospholipase Cγ were used to affinity purify proteins from brain extracts. The resulting protein complexes were screened for AKAPs by an overlay procedure using the radiolabeled regulatory subunit of PKA (RII) as a probe. An RII-binding protein of 84 kDa co-purified with the Abl kinase SH3 domain, but not other SH3 domains (Figure 1A). Control experiments confirmed that solid-phase binding of RII to the 'Abl-AKAP' was blocked in the presence of the anchoring inhibitor peptide, Ht31, which is an antagonist of RII–AKAP interactions (Figure 1B). This technique is used routinely as a first diagnostic to identify AKAPs (Carr and Scott, 1992).

Identification of the 'Abl-AKAP' involved a purification strategy that took advantage of its interaction with the SH3 domain of Abl (Figure 2A). Rat brain extract was incubated with the GST-tagged Abl SH3 domain immobilized on glutathione–Sepharose. Bound proteins were eluted with glutathione and fractionated by MonoQ anion exchange chromatography using a fast protein liquid chromatography (FPLC) system (Figure 2B). Fractions enriched for 'Abl-AKAP' were detected by RII overlay. A band of ~84 kDa that corresponded to the only RII-binding protein was enriched in fractions 13–16 (Figure 2C). This material was separated further by electrophoresis on a 4–15% SDS gel (Figure 2D), excised from the gel and subjected to trypsin cleavage. Three tryptic peptides sequenced by mass spectroscopy exhibited 100% identity with regions of a human cDNA clone, KIAA0269 (DDBJ/EMBL/GenBank accession No. D87459) (Nagase *et al*., 1996). Human and mouse cDNAs encoding this protein were generated by PCR and the mouse sequence (DDBJ/EMBL/GenBank accession No. AF290877) is presented in Figure 2E.

Recently, this protein was identified as Scar-1, the mammalian homolog of a *D.discoideum* protein that interacts with the p21 subunit of the Arp2/3 complex (Bear *et al*., 1998; Machesky *et al*., 1999), and WAVE-1, a WASP family member that associates with the actin cytoskeleton and is functionally coupled to the Rho family GTPase Rac (Miki *et al*., 1998; Suetsugu *et al*., 1999). In light of these observations, we will now refer to the 'Abl-AKAP' as WAVE-1.

WAVE-1 binds PKA and Abl kinase inside cells

To analyze further the properties of WAVE-1, a bacterial expression vector was generated by ligating the coding region of the human cDNA into the plasmid pEt30. Recombinant WAVE-1 protein migrated at 84 kDa on SDS–PAGE and bound to RII in the overlay assay (Figure 3A). These properties are consistent with the isolation of the Abl-interacting AKAP described above (Figures 1 and 2). In order to establish whether WAVE-1 bound to both PKA and Abl inside cells, a mammalian expression vector (pcDNA3) encoding WAVE-1 tagged with the FLAG epitope was transfected into HEK-293 cells. Lysates from control and transfected cells were subjected to immunoprecipitation with a monoclonal antibody against the FLAG epitope. Co-purification of the Abl tyrosine kinase was established by immunoblotting (Figure 3B, top panel). Co-precipitation of WAVE-1 and PKA was confirmed by RII overlay (Figure 3B, middle panel) and immunodetection of the catalytic subunit (Figure 3B, bottom panel). These results suggest that recombinant WAVE-1 can interact with endogenous Abl and PKA inside HEK-293 cells. More definitive experiments were conducted to establish whether endogenous WAVE-1 interacts with both kinases *in vivo*. Polyclonal antibodies raised against WAVE-1 detected a single band of ~84 kDa in rat brain extracts (Figure 3C) and immunoprecipitated an RII-binding protein of the same size from rat brain extracts (Figure 3D, middle panel). Co-purification of the Abl tyrosine kinase (Figure 3D, top panel) and the catalytic subunit of the PKA holoenzyme (Figure 3D, bottom panel) was confirmed by immunoblotting. WAVE-1, Abl or PKA were not detected when immunoprecipitations were performed with pre-immune serum (Figure 3D). Collectively, these results demonstrate that WAVE-1 serves as a scaffold to bind the PKA holoenzyme and the Abl tyrosine kinase in cells and tissues.

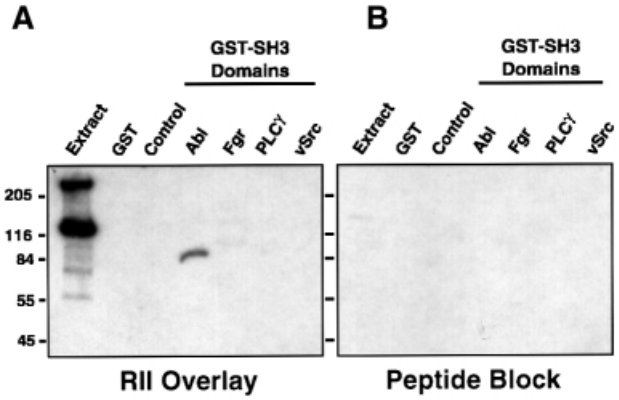

Fig. 1. Identification of an 84 kDa RII-binding protein that interacts with the SH3 domain of the Abl tyrosine kinase. Rat brain extracts were subjected to pull-down assays using GST fusion proteins expressing the SH3 domains from Abl kinase, the tyrosine kinase Fgr, phospholipase Cγ and the tyrosine kinase vSrc. Control experiments were performed using GST alone and an unrelated GST fusion protein, GST–PP2A/A. RII-binding proteins were detected by a solid-phase overlay assay (Hausken *et al*., 1998). Detection of immobilized radiolabeled RII was by autoradiogram in the absence (**A**) and in the presence (**B**) of RII blocking peptide Ht31 (1 μM). A representative blot from four individual experiments is presented. The source of the GST fusion protein is indicated above each lane. Molecular weight markers are indicated.

Mapping of the Abl kinase and PKA interaction domains on WAVE

A series of recombinant WAVE-1 fragments was generated to map the sites of interaction with the GST–SH3

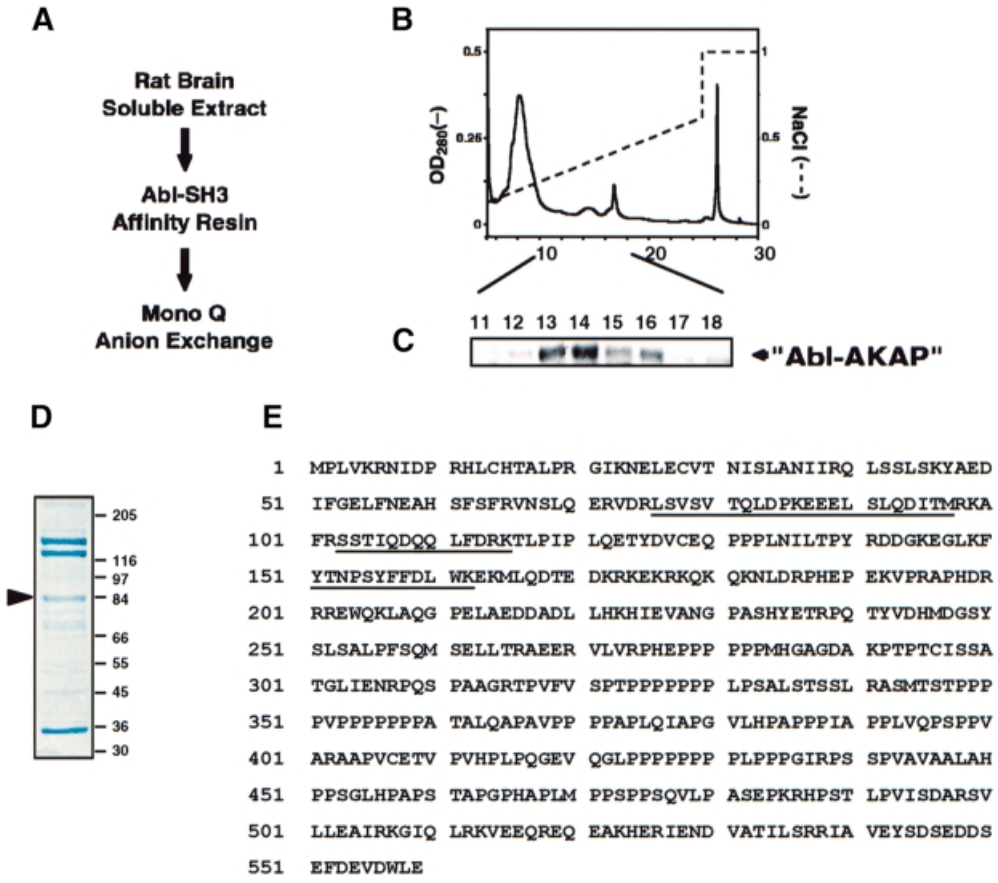

Fig. 2. Purification of the 84 kDa 'Abl-AKAP' RII-binding protein. (**A**) The 'Abl-AKAP' was isolated from rat brain extracts by a purification strategy that took advantage of its selective interaction with the SH3 domain of Abl. Eluates from the Abl SH3 affinity resin were applied to a MonoQ anion exchange column using FPLC. (**B**) Proteins were eluted from the MonoQ column with a linear gradient of NaCl and the fractions were analyzed for absorbance (OD_{280}). (**C**) The elution of the 84 kDa RII-binding protein was detected by RII overlay assay in fractions 12–16. (**D**) The peak fractions were pooled, concentrated, separated by SDS–PAGE and stained with Coomassie Blue dye. Molecular weight markers are indicated and the migration of the 'Abl-AKAP' is denoted by an arrow. This protein band was excised from the gel, fragmented by digestion with trypsin and subjected to microsequence analysis using a MALDI-TOF mass spectrometer. (**E**) BLAST sequence analysis of three peptides obtained from the mass spectrometry (underlined) identified WAVE-1. The mouse WAVE-1 sequence is presented.

domain of Abl tyrosine kinase (Figure 4A). Only fragments including residues 300–410 of WAVE-1 bound to the Abl SH3 domain, whereas fragments lacking this region or GST alone were unable to interact (Figure 4B). Controls confirmed that equivalent amounts of each GST–WAVE-1 fragment were used in these experiments (Figure 4C). It is well established that SH3 domains recognize a core PXXP motif (Pawson and Gish, 1992). Several polyproline stretches are present within this region of the WAVE-1 sequence that could participate in binding to the Abl SH3 domain (Figure 2E).

Biochemical and structural analyses have shown that the RII-binding domains of AKAPs involve a short amphipathic helix that provides extensive hydrophobic contact with a complementary region on the R subunit dimer (Carr *et al*., 1991, 1992; Newlon *et al*., 1999). Mapping studies suggested that a region between residues 480 and 520 of WAVE-1 contains determinants for PKA anchoring as fragments encompassing this region bound RII when a series of GST fusion proteins was screened by the overlay procedure (Figure 5B). On the basis of sequence similarity to other AKAPs and secondary structure predictions, residues 493–510 of WAVE-1 seemed likely to contain the principal determinants for RII binding (Figure 5A). Accordingly, substitution of isoleucines 505 and 509 by proline abolished RII interaction as assessed by the RII overlay (Figure 5C). These mutations correspond to changes in other AKAPs that disrupt interaction with RII (Carr *et al*., 1991; Hausken *et al*., 1996), thus suggesting that WAVE-1 is an AKAP. More conclusive evidence was provided by enzymological studies showing that immunoprecipitation of recombinant WAVE-1 from HEK-293 cells resulted in a 5.1 $\pm$ 0.6-fold (n = 3) enrichment in PKA activity (Figure 5D). All kinase activity was blocked by the PKI 5–24 peptide, a specific inhibitor of PKA (Scott *et al*., 1985). Collectively, these data confirm that WAVE-1 functions as a conventional AKAP inside cells.

Recently, two additional WAVE isoforms, WAVE-2 and WAVE-3, have been identified (Suetsugu *et al*., 1999). Alignment of all three sequences revealed considerable homology within the putative RII-binding domain, although certain key hydrophobic residues were not conserved in WAVE-2 and WAVE-3 (Figure 5E). WAVE-2 and WAVE-3 cDNAs were isolated by RT–PCR, expressed in bacteria and purified in order to

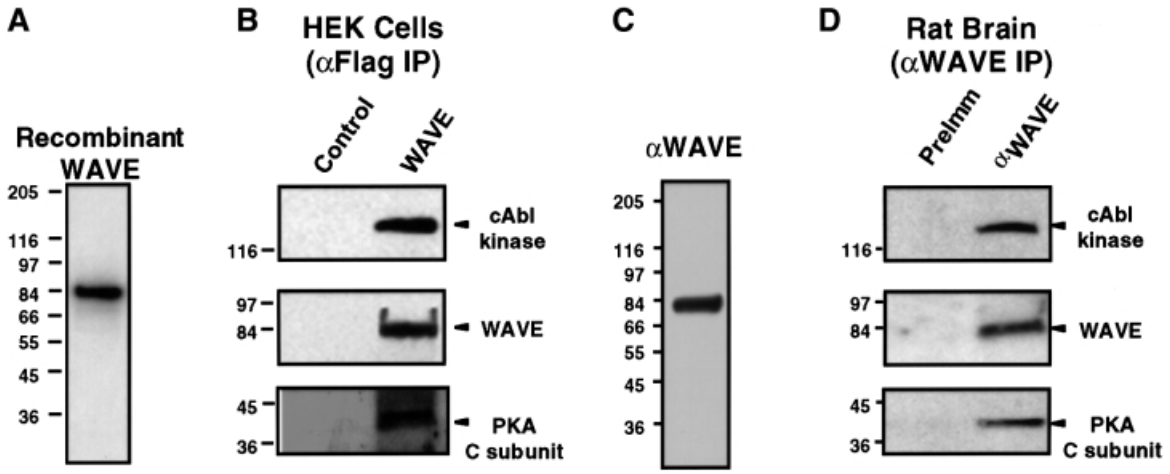

Fig. 3. PKA and Abl interact with WAVE inside cells. (**A**) WAVE-1 protein epitope tagged with the His_6 sequence was expressed in bacteria. Expression of the recombinant protein was detected by the RII overlay assay as described in Materials and methods (Hausken *et al*., 1998). Molecular weight markers are indicated. (**B**) Cell extracts prepared from HEK-293 cells expressing recombinant WAVE-1 epitope tagged with the FLAG sequence were subjected to immunoprecipitation using a monoclonal antibody against the FLAG epitope. Control immunoprecipitations were performed with the same antibody using cell extracts prepared from non-transfected HEK-293 cells. Co-purification of Abl kinase (top panel), WAVE (middle panel) and the catalytic subunit of the PKA holoenzyme (bottom panel) were detected by immunoblot using specific antibodies against each protein. Molecular weight markers are indicated. Arrowheads denote the migration position of each protein. (**C**) Rat brain extracts were immunoblotted with affinity-purified antibodies to WAVE. Molecular weight standards are indicated. (**D**) Rat brain extracts were subjected to immunoprecipitation using the affinity-purified WAVE antibodies. Co-purification of Abl kinase (top panel), WAVE (middle panel) and the catalytic subunit of the PKA holoenzyme (bottom panel) detected by immunoblotting using specific antibodies against each kinase and RII overlay for WAVE-1. Molecular weight standards are indicated. Arrowheads denote the migration position of each protein. Representative examples of three individual experiments are presented.

determine whether the other WAVE isoforms were AKAPs. Neither WAVE-2 nor WAVE-3 bound RII as assessed by the RII overlay assay (Figure 5F, top panel). Control experiments confirmed that equivalent amounts of each WAVE isoform were used (Figure 5F, bottom panel). To assess the ability of each WAVE form to interact with the PKA holoenzyme inside cells, HEK-293 cells were transfected with FLAG-tagged vectors encoding the individual WAVE isoforms. Cell extracts were immunoprecipitated using a monoclonal antibody against the FLAG epitope. The catalytic subunit of PKA was only detected in immunoprecipitates from cells expressing WAVE-1 (Figure 5G, top panel). Control experiments confirmed that equivalent amounts of each WAVE isoform were immunoprecipitated (Figure 5G, bottom panel). Collectively, these data indicate that WAVE-1 is the only isoform that binds RII and serves to anchor PKA.

Interestingly, the RII-binding region of WAVE-1 overlaps with a VPH domain (residues 493–510, Figure 6A) that has previously been characterized as a binding site for G actin (Machesky and Insall, 1998). To refine the region on WAVE-1 responsible for interaction with G actin, a mutant was constructed in which Arg512 and Lys513 were mutated to glutamate (Figure 6A). Analogous mutations in the actin-binding protein verprolin disrupt interaction with actin (Vaduva *et al*., 1997). Likewise, the WAVE-1 R512E, K513E mutant did not bind to G actin (Figure 6B), although it retained some ability to interact with RII as assessed by the overlay assay (data not shown). These results suggest that the G actin- and RII-binding sites overlap in WAVE-1 but that each protein recognizes distinct determinants within the 493–510 sequence. To determine whether WAVE-1 could bind to both RII and G actin, a GST fusion of WAVE (residues 480–559) was incubated with recombinant RII in the presence of increasing amounts of actin extracts (Figure 6C). Actin binding and RII binding were assessed by immunoblotting. Increased actin binding (Figure 6C, top panel) corresponded to decreased RII interaction (Figure 6C, middle panel) with the WAVE fusion protein (Figure 6C, bottom panel). These data suggest that RII and actin binding to WAVE-1 are mutually exclusive.

Immunocytochemical localization of the WAVE signaling complex in Swiss 3T3 fibroblasts

Immunocytochemical analysis of the WAVE signal transduction complex was performed in Swiss 3T3 fibroblasts (Figure 7A–D). WAVE staining was detected in the nucleus and at focal adhesions, specialized structures that attach the actin cytoskeleton to membranes (Figure 7A). Two separate antibodies raised against recombinant WAVE-1, VO59 and VO60, gave identical staining patterns. Intracellular pools of WAVE were confirmed by immunofluorescent detection of paxillin as a marker for focal adhesions (Figure 7B and D) and counterstaining with Hoechst dye to detect DNA as a nuclear marker (Figure 7C and D).

WAVE acts downstream of PDGF receptor activation where it is functionally coupled to a Rho family GTPase, Rac (Nobes *et al*., 1995). Therefore, experiments were initiated to investigate the subcellular location of WAVE, PKA and Abl during Rac-induced reorganization of actin. It was important to establish that WAVE-1 was expressed in these fibroblasts. In the absence of isoform-specific antibodies, we detected WAVE-1 on the basis of its PKA-anchoring properties (Figure 8A and B). These experiments confirm that WAVE-1 is expressed in Swiss 3T3 fibroblasts.

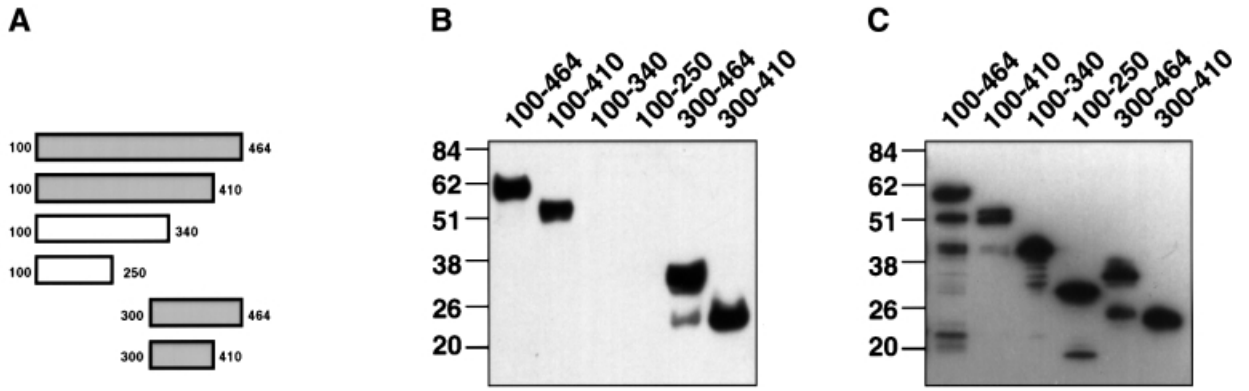

Fig. 4. Mapping the Abl-binding domain. (**A**) A schematic representation of recombinant His-tagged WAVE-1 fusion fragments used in mapping studies is presented. Fragments that interact with the GST–SH3 domain from Abl (filled boxes) and fragments negative for binding (open boxes) are indicated. The first and last residues in each fragment of WAVE-1 are numbered. (**B**) Recombinant fragments of WAVE-1 were incubated with GST–Abl SH3 fusion protein that was immobilized to glutathione–Sepharose for 1 h at 4°C. Bound proteins were detected by immunoblotting using a monoclonal antibody to the histidine tag present on the WAVE fragments. (**C**) A control immunoblot indicating the expression levels of each His-tagged WAVE-1 fragment loaded onto the GST–Abl SH3 domain column. WAVE-1 fragments were detected by immunoblotting using a monoclonal antibody to the histidine tag. Molecular weight standards are indicated. Representative examples of three individual experiments are presented.

Control and PDGF-treated (10 ng/ml) cells were stained with affinity-purified antibodies against WAVE (green) and murine RII (blue), while actin was detected with Texas red–phalloidin (red). All three proteins exhibited distinct subcellular distributions in cells not treated with PDGF (Figure 8C–F). WAVE was detected in the nucleus and at focal adhesions (Figure 8C), actin was aligned along stress fibers (Figure 8D) and RII was predominantly perinuclear (Figure 8E). The signals for WAVE and actin overlapped at focal adhesions, but there was no detectable RII signal at these sites (Figure 8F). In contrast, treatment with PDGF promoted distinct changes in the staining pattern of all three proteins (Figure 8G–J). PDGF promoted the formation of lamellipodia and a 'ring structure' at internal sites of actin reorganization (Figure 8H). PDGF also reduced the number of focal adhesions (although some cells were less robust in their response to PDGF than others) (data not shown). WAVE staining, however, was clearly evident at sites of actin reorganization (Figure 8G). Likewise, a significant proportion of the RII signal was now detected at sites of actin reorganization (Figure 8I). A composite image shows that all three signals overlap in the same focal plane, suggesting that all three proteins are co-localized (Figure 8J). Treatment with the actin-depolymerizing agent, cytochalasin D, abolished the 'ring structure' formed in response to PDGF and prevented the movement of WAVE and RII (Figure 8K–N). These findings lend further support to our biochemical evidence demonstrating that WAVE binds to PKA or actin.

Similar experiments were repeated to demonstrate that WAVE (green), Abl (red) and RII (blue) move to similar 'ring structures' upon PDGF treatment of Swiss 3T3 fibroblasts (Figure 9A–H). As reported previously, Abl was also detected throughout the cytoplasm and within the nucleus (McWhirter and Wang, 1991; Pendergast, 1996). Interestingly, other studies have suggested that Abl may also be found within focal adhesions where Abl is thought to phosphorylate paxillin (Lewis and Schwartz, 1998). Although the Abl and PKA signals appeared to be more prominent in the PDGF-treated cells, we believe that this represents the increased surface area of the signal at these regions. These findings imply that extracellular stimuli that promote Rac activation result in the movement of WAVE, PKA and Abl to sites of cytoskeletal reorganization.

Recombinant WAVE isoforms co-immunoprecipitate

Our immunocytochemical analysis indicated that WAVE and PKA were recruited to the sites of actin reorganization (Figures 8 and 9). Yet our *in vitro* binding studies suggested that actin and RII bind WAVE-1 in a mutually exclusive manner (Figure 6). Therefore, it was unclear how movement of WAVE-1 to sites of actin reorganization could also promote the translocation of RII. One potential explanation was that WAVE-1 could complex with other WAVE isoforms. To test directly whether interactions could occur, HEK-293 cells were transfected with different combinations of FLAG- and green fluorescent protein (GFP)-tagged WAVE isoforms. Immunoprecipitation of WAVE-1 with antibodies to the FLAG epitope resulted in the co-precipitation of the GFP–WAVE-1, GFP–WAVE-2 or GFP–WAVE-3 fusion proteins, respectively (Figure 10). These data demonstrate that WAVE isoforms can be recruited into larger complexes.

Discussion

Remodeling of the actin cytoskeleton orchestrates cellular events including cell shape, polarity, phagocytosis, motility and cytokinesis. In each case, the coordinated assembly and disassembly of actin is tightly regulated by different combinations of signal transduction enzymes. Although the precise molecular mechanisms underlying these processes are still being elucidated, it is already apparent that the Wiskott–Aldrich syndrome proteins WASP, N-WASP and WAVE are downstream targets for individual Rho family GTPases. It is believed that this family of adaptor proteins funnels signals from heptahelical or growth factor receptors to sites of actin reorganization through association with a variety of

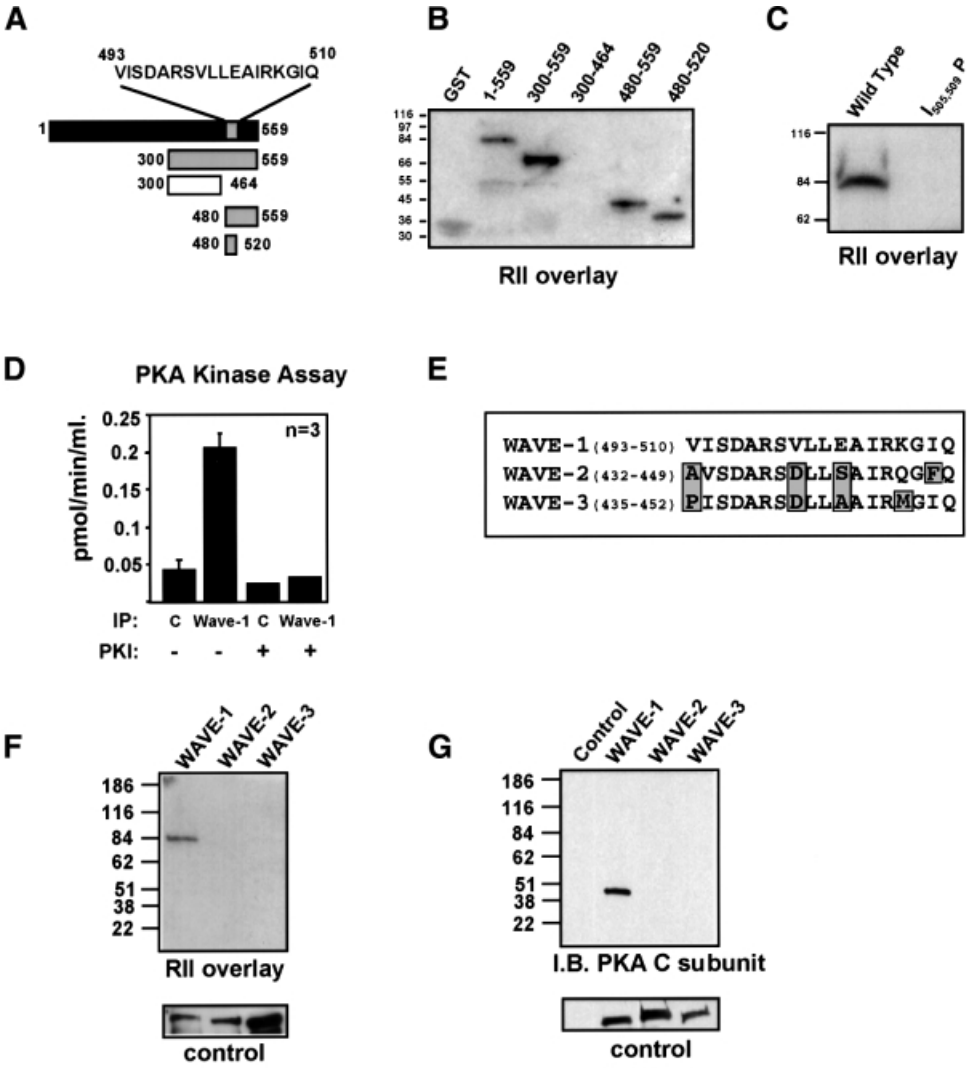

Fig. 5. Mapping the RII-binding domain. (**A**) A schematic representation of recombinant WAVE fragments used for the mapping of the RII-binding site. Fragments that interact with RII (filled boxes) and fragments negative for binding (open boxes) are indicated. The first and last residues in each fragment of WAVE-1 are numbered. The amino acid sequence of the putative RII-binding site, which is located between residues 493 and 510 of WAVE-1, is indicated using the one letter code. (**B**) Fragments of WAVE-1 were separated by electrophoresis on a 6% SDS–polyacrylamide gel, electrotransferred to nitrocellulose and assayed for RII binding by overlay assay (Hausken *et al*., 1998). Detection of immobilized RII was by autoradiography. Molecular weight standards are indicated. (**C**) Point mutations were introduced at positions 505 and 509 of the WAVE-1 protein. The RII-binding characteristics of the wild-type and mutant proteins (indicated above each lane) were assessed by the overlay assay (Hausken *et al*., 1998). (**D**) Recombinant WAVE-1 was immunoprecipitated from HEK-293 cell lysates using a monoclonal antibody against the FLAG epitope. Control (C) immunoprecipitations were performed with cells not transfected with WAVE-1. Co-purification of the PKA holoenzyme was measured by assaying for the catalytic subunit of PKA using a filter paper assay (Corbin and Reimann, 1974). PKA-specific activity was measured as pmol/min/ml of material. PKA activity was blocked by the specific inhibitor PKI 5–24 peptide. The data represent the results of three independent experiments. (**E**) The RII-binding region of WAVE-1 is aligned with corresponding regions in the WAVE-2 and WAVE-3 isoforms. Residues are presented using the one letter code. The first and last amino acids in each sequence are indicated. Amino acids not conserved in WAVE-2 and WAVE-3 are boxed and shaded. (**F**) His epitope-tagged WAVE-1, WAVE-2 and WAVE-3 were expressed and purified from bacteria. Soluble extracts were separated by electrophoresis on a 6% SDS–polyacrylamide gel, electrotransferred to nitrocellulose and assayed for RII binding by overlay assay (top panel) (Hausken *et al*., 1998). The expression level of each WAVE isoform was detected by western blotting using the anti-His antibody (bottom panel). Molecular weight standards are indicated. Representative examples of three individual experiments are presented. (**G**) Soluble extracts from HEK-293 cells transfected with FLAG-tagged WAVE-1, WAVE-2 or WAVE-3 and pcDNA3 vector alone (control) were immunoprecipitated using a monoclonal antibody against the FLAG epitope. Co-precipitation of the PKA catalytic subunit (top panel) was detected by immunoblotting using a monoclonal antibody against the kinase. The expression level of each WAVE isoform (bottom panel) was monitored by western blotting using the anti-FLAG monoclonal antibody. Representative examples of three individual experiments are presented.

actin-binding proteins and the Arp2/3 complex. Our biochemical studies now highlight a previously unrecognized role for the WAVE-1 isoform as a kinase-anchoring protein that binds PKA and the tyrosine kinase c-Abl. This provides a mechanism whereby a second messenger-dependent serine/threonine kinase and a non-receptor tyrosine kinase are directed to sites of actin reorganization.

We originally identified WAVE in a screen for brain AKAPs that interact with isolated SH3 domains from a variety of signal transduction molecules. This method proved to be surprisingly stringent as parallel approaches using SH3 domains from the related non-receptor tyrosine kinases Src and Fgr were negative for WAVE binding. In contrast, WASP may have a more generalized kinase-

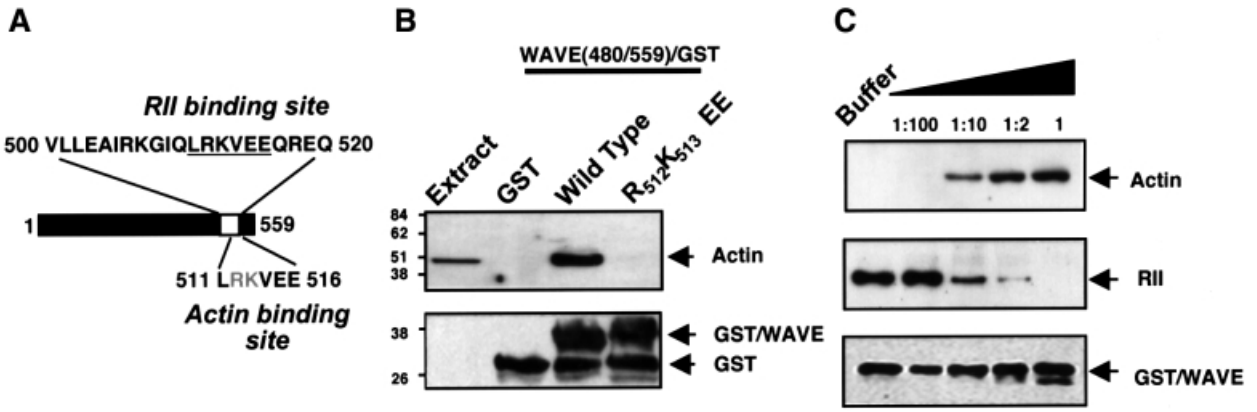

Fig. 6. RII and actin binding to WAVE is mutually exclusive. (**A**) Schematic representation of RII- (upper sequence) and actin-binding sites (lower sequence) on WAVE-1. Amino acids are presented using the one letter code. The first and last residues are numbered. (**B**) Solution-phase binding of GST–WAVE-1 and mutants (indicated above each lane) to actin was detected by immunoblotting (top panel) with a polyclonal antibody against rat actin. The expression level of each GST fusion protein (bottom panel) was confirmed by immunoblotting using monoclonal antibodies against GST. Molecular weight markers are indicated. (**C**) Solution-phase competition assay was used to examine actin displacement of RII–WAVE-1 binding. The WAVE-1–RII complex was formed on GST–beads and incubated with increasing concentrations of rat brain extract (indicated above each lane). Bound actin (top panel) and RII (middle panel) were detected by immunoblotting with polyclonal antibodies against each protein. Equal levels of the WAVE-1 fragment were detected by immunoblotting using affinity-purified anti-WAVE antibody.

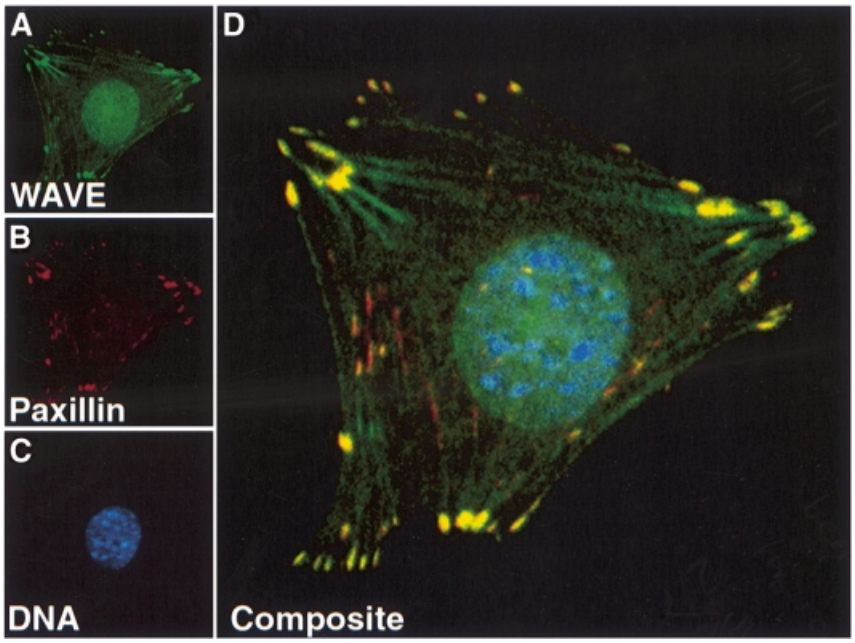

Fig. 7. The subcellular distribution of WAVE. Confocal microscopy of Swiss 3T3 fibroblasts demonstrating the subcellular distribution of endogenous WAVE and cellular markers. Immunocytochemical analysis was carried out using a polyclonal antibody against (**A**) WAVE (green), (**B**) a monoclonal antibody against paxillin, a marker for focal adhesions (red), and (**C**) the nucleus was detected by DNA staining with Hoechst dye (blue). (**D**) A merged image depicts the distribution of all three stains. Control immunocytochemical analysis showed no antibody signal.

anchoring role as it interacts with the SH3 domains of Src, Fgr, Fyn and the Tec tyrosine kinases, Btk and Itk (Bunnell *et al*., 1996; Cory *et al*., 1996; Finan *et al*., 1996; Kinnon *et al*., 1997; Banin *et al*., 1999). Structure–function analysis and screening of combinatorial peptide libraries have defined minimal core recognition motifs for a number of SH3 domains (Pawson and Gish, 1992). The Abl SH3 domain is distinct as it prefers the sequence P**P**X{F,Y,W}XP**P**P{L,I,V,G,A}**P** (bold residues are highly conserved) (Sparks *et al*., 1996). Perhaps the closest homology to an Abl-binding consensus sequence with the region of WAVE-1 defined by our mapping studies lies between residues 317 and 325 (**P**VFVS**P**TP**P**). Abl binding appears to be a common feature of the WAVE family as recombinant WAVE-2 and WAVE-3 also interact with the Abl SH3 domain *in vitro* (R.S.Westphal and J.D.Scott, unpublished observation).

In contrast, PKA anchoring does not appear to be a generalized feature of all WAVE isoforms. Only WAVE-1 binds RII *in vitro*, and immunoprecipitation of recombinant WAVE-1 from cell lines results in a 5-fold enrichment of endogenous PKA activity. Sequence alignments indicate that WAVE-2 and WAVE-3 lack certain key hydrophobic side chains that are required to bond with

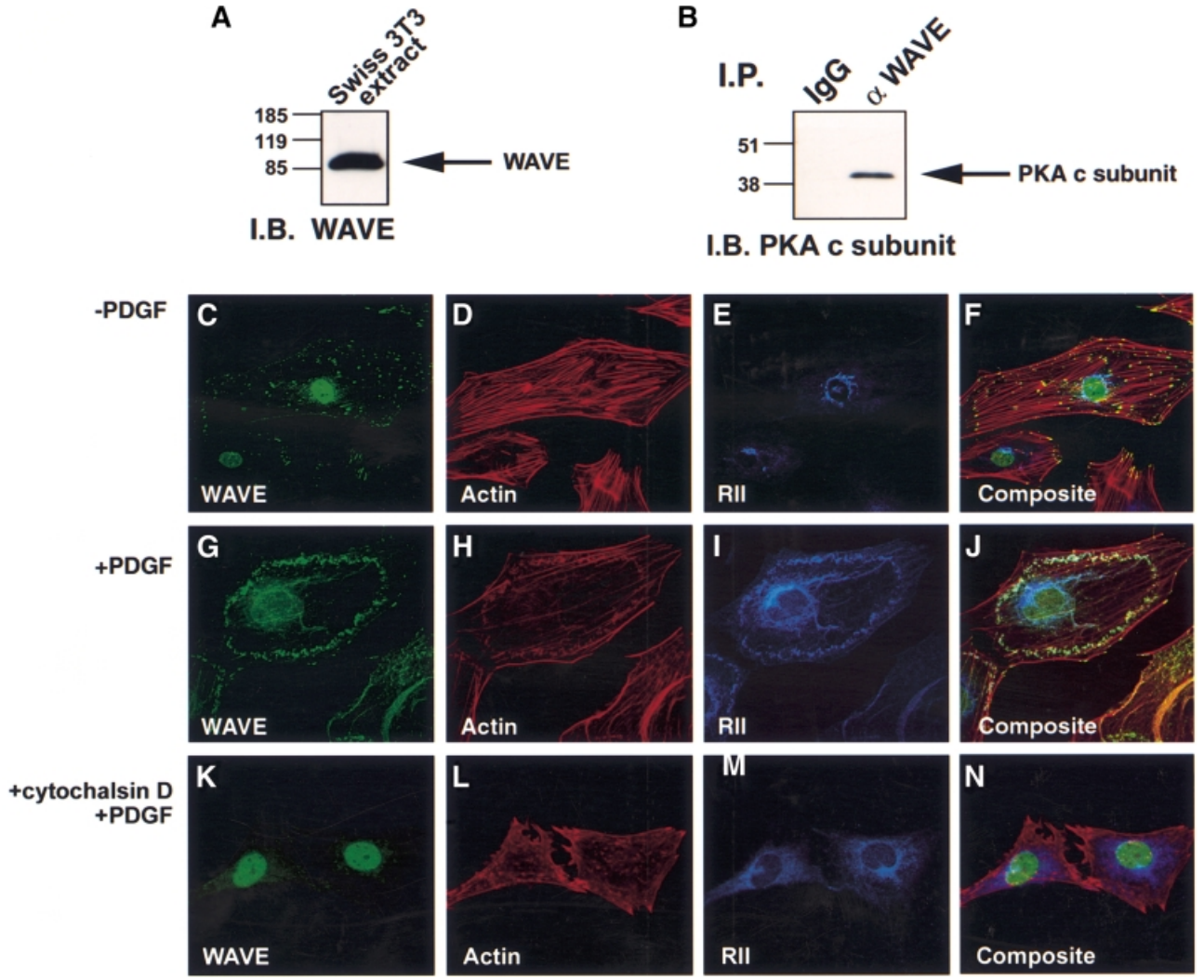

Fig. 8. Dynamic assembly of the WAVE-1–PKA complex in response to PDGF. (**A**) Cell lysates prepared from Swiss 3T3 fibroblasts were probed for the expression of endogenous WAVE. WAVE was detected by immunoblotting using polyclonal antibodies. Molecular weight markers are indicated. The arrow indicates the migration position of WAVE. (**B**) Polyclonal antibodies were used to immunoprecipitate endogenous WAVE from Swiss 3T3 fibroblast extracts. Co-precipitation of the PKA holoenzyme was confirmed by immunodetection of the PKA catalytic subunit using monoclonal antibodies. The arrow indicates the migration position of the catalytic subunit. Molecular markers are indicated. Experiments were conducted at least three times. (C–N) Confocal microscopy of Swiss 3T3 fibroblasts demonstrating the subcellular distribution of WAVE and its binding partners. Immunocytochemical analysis was carried out (**C**, **G** and **K**) using a rabbit polyclonal antibody against WAVE (green), (**D**, **H** and **L**) Texas red–phalloidin to detect actin (red) and (**E**, **I** and **M**) mouse monoclonal RII (blue). Merged images (**F**, **J** and **N**) depict the subcellular distribution of all three stains. The cells in (C–F) were serum starved. The cells in (G–J) were treated with PDGF (10 ng/ml) for 10 min prior to fixation. Cells in (K–N) were treated with cytochalasin D (10 μM) for 30 min prior to PDGF (10 ng/ml) for 10 min, and then fixed. Control immunocytochemical analysis showed no antibody signal.

a binding surface formed by the RII dimer (Figure 5C). Although only WAVE-1 can function as an AKAP, its ability to complex with other WAVE isoforms has the potential to increase the representation of protein kinases within the complex. Another unique feature of the PKA–WAVE-1 interaction is that actin may compete for the RII-binding site. Although the physiological significance of these interactions is not yet clear, our data provide the first evidence for the regulation of an RII–AKAP interaction by another protein. The high intracellular concentration of actin may well be sufficient to compete with the RII–WAVE-1 interaction as AKAP–RII binding typically occurs in the nanomolar range (Carr *et al.*, 1992; Herberg *et al.*, 2000). Thus, PKA anchoring may be regulated dynamically at sites of actin reorganization.

Although we present evidence that RII and actin compete for WAVE-1 binding, our immunocytochemical experiments paradoxically suggest that WAVE and PKA are recruited to lamellipodia and actin ring structures in response to PDGF treatment. There are three possible explanations for this apparent contradiction. First of all, distinct pools of WAVE associated with actin or PKA could exist at sites of actin remodeling. Secondly, other actin-binding proteins within the WAVE-1 signaling complex such as profilin, the Arp2/3 complex or Abl may contribute to the targeting function. Potentially, this high degree of cross-linking to the cytoskeleton may explain why we have been unable consistently to demonstrate increased PKA or Abl activity associated with WAVE imunoprecipitated from PDGF-treated fibroblasts.

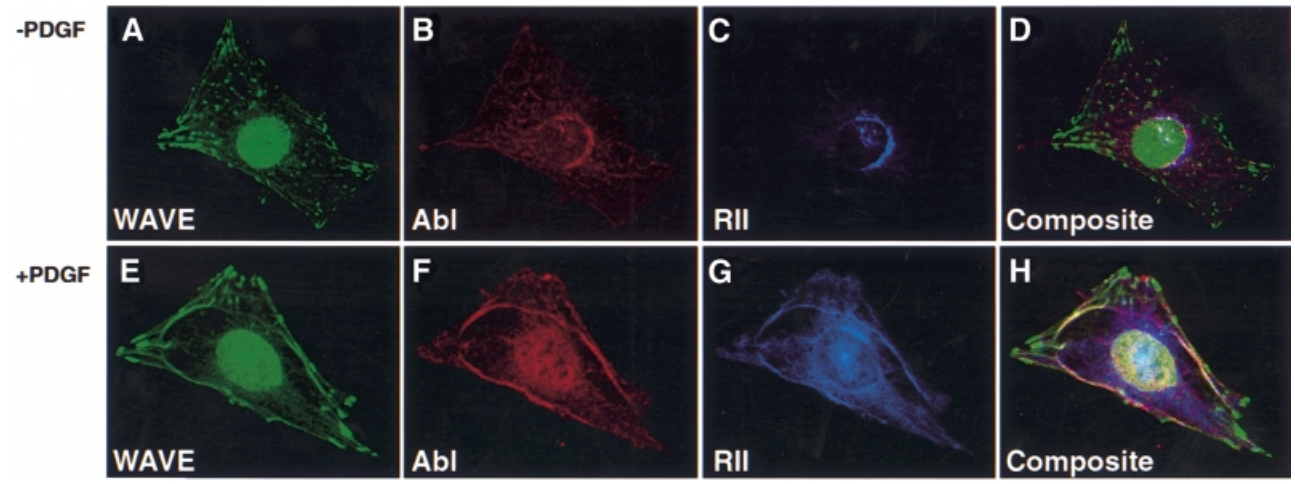

Fig. 9. Dynamic assembly of the WAVE/Abl/PKA signaling scaffold in response to PDGF. Immunocytochemical analysis was carried out (**A** and **E**) using a rabbit polyclonal antibody against WAVE (green), (**B** and **F**) mouse monoclonal antibody against Abl (red) and (**C** and **G**) goat polyclonal antibody to RII (blue). Merged images (**D** and **H**) depict the subcellular distribution of all three proteins. The cells in (A–D) were serum starved. The cells in (E–H) were treated with PDGF (10 ng/ml) for 10 min prior to fixation. Control immunocytochemical analysis showed no antibody signal.

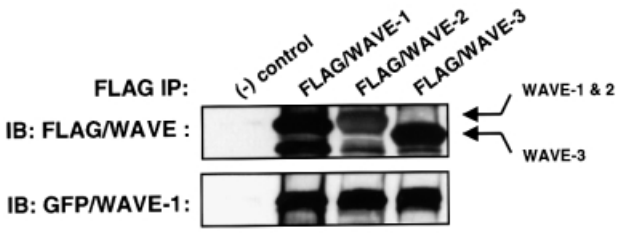

Fig. 10. Oligomerization of WAVE isoforms. HEK-293 cells expressing GFP-tagged WAVE-1 or control vector were co-transfected with FLAG-tagged WAVE-1, WAVE-2 or WAVE-3 (indicated above each lane). Soluble HEK-293 cell extracts were subjected to immunoprecipitation using an anti-FLAG monoclonal antibody. Expression of each WAVE isoform (top panel) was confirmed by immunoblotting with monoclonal antibodies against the FLAG epitope. The migration positions of each WAVE isoform are indicated by arrows. Co-precipitation of GFP-tagged WAVE-1 was detected by immunoblotting using antibodies against GFP (bottom panel).

This is a reasonable explanation given the possibility for multiple sites of contact between the WAVE signaling complex and other actin-binding proteins. A third explanation is suggested by our data demonstrating additional interactions between WAVE isoforms. This finding is consistent with recent cross-linking studies suggesting that N-WASP forms homodimers (Carlier *et al*., 2000). Future studies are planned to define the mechanism of WAVE–WAVE interactions and to delineate between the formation of hetero- or homomultimers or the recruitment of WAVE isoforms into a multiprotein complex through association with intermediary proteins. Thus, a WAVE-1–PKA complex could be tethered to the cytoskeleton through actin-based interactions provided by either WAVE-2 or WAVE-3. This more sophisticated level of molecular organization undoubtedly has implications for WAVE signaling.

Functional studies implicate cyclic nucleotide-dependent protein kinases and Abl kinases in the control of processes driven by actin dynamics, including axonal outgrowth or growth cone guidance. For instance, in *Xenopus* spinal neurons, cAMP-dependent activity regulates the choice of growth cone attraction and repulsion in response to brain-derived neurotrophic factor (BNDF) or acetylcholine (Song *et al*., 1997). Importantly, PKA activity levels determine whether the response is attraction or repulsion, as specific inhibitors of PKA can convert an attractant such as BNDF to a repellent, suggesting that both growth cone attraction and repulsion are controlled by PKA (Ming *et al*., 1997). Interestingly, Abl also participates in the regulation of axonal guidance pathways. Candidate Abl substrates include *disabled* and the neuronal receptor protein tyrosine phosphatase *Dlar*, which are essential genes for axonal guidance in *Drosophila* (Gertler *et al*., 1993; Wills *et al*., 1999). In addition, screens for modulators of Abl null phenotypes have also identified other Abl substrates and regulators of the actin cytoskeleton including *enabled* (also called Mena in mouse), which binds to profilin (Gertler *et al*., 1995; Ahern-Djamali *et al*., 1999). These observations are in keeping with our hypothesis that WAVE-1 functions to maintain PKA and Abl at sites of actin reorganization. Presumably this level of organization provides a mechanism to facilitate the rapid changes in cytoskeletal architecture that emanate from activation of Rac. Furthermore, the dynamic nature of the interactions suggests that extracellular effectors such as PDGF may transiently promote the assembly of an actin-based transduction unit at sites of actin remodeling. Future studies will probably focus on identifying additional components of the WAVE complex and defining particular substrates for both PKA and Abl kinases.

Materials and methods

Preparation of tissue and cell extracts

Soluble tissue extracts were prepared from frozen rat brains (Pel Freeze) by dounce homogenization in lysis buffer [25 mM HEPES, 150 mM NaCl, 0.5% Triton, 1 mM EDTA, 1 mM 4-(2-aminoethyl)-benzenesulfonyl fluoride, 1 mM benzamidine, 2 μg/ml pepstatin and 2 μg/ml leupeptin] and centrifugation at 38 000 *g* for 1 h at 4°C. Cell extracts were prepared by washing cells with phosphate-buffered saline (PBS),

followed by scraping adherent cells in 1 ml of lysis buffer, incubating on ice for 15 min and then centrifuging at 15 000 *g* for 30 min. Extracts were prepared from the supernatants of each spin.

Purification of 'Abl-AKAP'

Soluble extract from five frozen rat brains was incubated with 500 µl of GST–Abl SH3 domain fusion protein (~0.5–2 mg) immobilized on glutathione–Sepharose (Pharmacia) overnight at 4°C. Precipitated resin was washed with lysis buffer and bound proteins were eluted with glutathione (15 mM) in anion exchange buffer (50 mM Tris pH 7.4, 1 mM EDTA). The eluted material was applied to a MonoQ anion exchange column using FPLC (Pharmacia). The column was developed with a linear gradient of NaCl (0–0.5 M) and fractions were assayed for the presence of the 84 kDa RII-binding protein by RII overlay assay. The pooled materials from three peak fractions were collected and concentrated. Samples were separated by SDS–PAGE (6% acrylamide) and stained with Coomassie Blue. A single protein band of 84 kDa was excised from the gel and subjected to peptide microsequencing using mass spectrometry (Harvard Microchem).

Primers used

All of the PCR primers used in this study are listed below.

Human WAVE-1 primers: AA3p1 (ggggatactgctaaacattcaaataaggcaag); Abl-Akap5p1(ctcttgcacttgcggatcctgaactggaataacga); and AAS129 (ggccgagctctcatgccgctagtgaaaagaaacatcgatcctagg).

Human WAVE-2 primers: W2/1AS (aagcaggtcgctacgggcatcgctgattacaggtagggttgatggatggcg); WAVE2S1 (gccgccatggatgccgttagtaacgaggaacatcgagccaaggcac); and W2AS1497F (gccgctcgagttaatcggaccagtcgtcctcatcaaattcagagg).

Human WAVE-3 primers: W3ASRT (gcacaatttgctatgtttagtggcacttaag); WAVE3S1 (gccggtcgacatgcctttagtgaagaggaacattgagccccggcac); WAVE3.S499 (caggacacagaagacaaaaggaaagagaaaaggcgt); W3AS1509 (gccgctcgagtcagtcggaccagtcgttctcgtcgaactctgagtc); and W3AS753 (cgggtaagagtaatccgtaacgtccgatgc).

Mouse WAVE-1 primers: WV.AS1 (gtcagcgtcatcctcagccagctctggac) and WV1.S1 (atgccgctagtgaaaagaaacatcgat).

RT–PCR and construction of cDNA expression plasmids

Human brain poly(A) RNA (Clontech) was used for preparation of WAVE-1, -2 and -3 cDNA using Superscript Choice System for cDNA synthesis (Gibco-BRL). WAVE-1, -2 and -3 cDNAs were PCR amplified using oligonucleotides containing restriction enzyme sites selected for each WAVE isoform. PCR products were digested with restriction enzymes and subcloned into the pet30a bacterial expression vector (Novagen). Subcloning of human WAVE-1, -2 and -3 into expression vectors encoding N-terminal FLAG tag (FLAG-pCDNA-3; kind gift from Dr Phillip Stork, Vollum Institute, Portland, OR), N-terminal GFP (pEGFP-C1; Clontech), N-terminal histidine tag (pet30a; Novagen) and GST (pGEX-4T1; Pharmacia) was performed following standard restriction digestion and ligation protocols. The sequence of all WAVE constructs was confirmed by DNA sequencing. The N-terminus of mouse WAVE-1 was cloned by rapid amplification of cDNA ends (RACE) using mouse brain marathon-adapted cDNA (Clontech), Advantage polymerase mix (Clontech) and primers WV.AS1 and WV1.S1. The C-terminus of mouse WAVE-1 was cloned from an expressed sequence-tagged clone (DDBJ/EMBL/GenBank accession No. Ai037400).

Purification of recombinant proteins

Fragments of WAVE cDNAs were expressed as N-terminal His_6-tagged fusions and as N-terminal GST fusions in bacteria (BL21DE3). Recombinant proteins expressed in bacteria were purified using either glutathione–Sepharose (Amersham Pharmacia Biotech) or hi-trap chelating resin (Amersham Pharmacia Biotech). Bacterial extracts containing GST fusion proteins were prepared by centrifugation of bacterial cultures, lysis of pelleted bacteria in PBS containing 2% sarcosyl, sonication and centrifugation at 38 000 *g* for 30 min at 4°C. Triton X-100 (4%) was added to the supernatant and the extract was incubated with glutathione–Sepharose (Pharmacia) overnight. The resin was washed with 10 bed volumes of PBS and stored at 4°C. Protein concentrations of bound GST fusion proteins were estimated by Coomassie staining of SDS–polyacrylamide gels. His_6-tagged fusion proteins were purified from bacterial extracts expressing the fusion proteins by urea extraction of bacterial cell pellets. Briefly, cells were pelleted by centrifugation at 5000 *g* for 10 min, then sonicated in buffer A at 4°C (20 mM HEPES, 6 M urea, 500 mM NaCl pH 7.9) and finally centrifuged at 35 000 *g* at 4°C for 30 min. The pellet was then sonicated in buffer A and centrifuged at 38 000 *g* for 60 min. Supernatants were filtered (0.2 µm) and then applied to hi-trap chelating resin (Pharmacia) using FPLC. Bound proteins were eluted with a stepwise gradient of imidazole (0–0.5 M) in buffer A without urea. Fractions containing purified protein were identified by Coomassie staining of SDS–polyacrylamide gels.

GST pull-down assays

GST fusion proteins (typically 20–40 µl of resin) were incubated with rat brain soluble extracts overnight at 4°C, washed with lysis buffer five times (1 ml volume) for 10 min and eluted with Laemmli sample buffer. In assays with recombinant His_6-tagged proteins, incubation with the GST fusion was for 2 h at 4°C followed by the same wash and elution protocol. Eluted proteins were analyzed by SDS–PAGE and immunoblotting.

Actin–RII competition assays

A 5 µl aliquot of GST–WAVE-1 (amino acids 480–559) and 15 µg of recombinant RII were incubated with 200 µl of actin-containing soluble rat brain extract or diluted actin containing soluble rat brain extract overnight at 4°C. Following the competition incubation, each sample was washed four times in 1 ml of lysis buffer plus once in lysis buffer containing 1 M NaCl and 1% Triton X-100. Samples were eluted with Laemmli sample buffer and split between two SDS–polyacrylamide gels. Western blotting was performed for either actin or RII on each gel. These blots were then stripped (in 0.2 M glycine, 0.1% Tween pH 2.5 for 20 min) of bound antibodies and reprobed for GST–WAVE using affinity-purified WAVE antibody to ensure equal loading.

Transfection of HEK-293 cells

HEK-293 cells at 50–75% confluence were transfected using lipofectamine PLUS (Gibco-BRL) according to the manufacturer's instructions. Cells were harvested 24 h post-transfection.

Generation of anti-WAVE antibodies and affinity purification

Antibodies to WAVE-1 were generated in two rabbits using recombinant His_6-tagged WAVE-1 (1–559) as the immunogen (Covance), resulting in two antibody preparations, VO59 and VO60. For affinity purification, the immunogen was immobilized on resin (Affi-Gel 15) and incubated overnight at 4°C with diluted WAVE antiserum [1:1 in Tris-buffered saline (TBS)]. The affinity resin was washed sequentially with 10 ml of TBS, 10 ml of TBS containing 1 M NaCl, and 10 ml of TBS. Bound antibodies were eluted with 0.2 M glycine pH 2.5 and collected in an equal volume of 1 M Tris pH 7.5. Eluted antibodies were then dialyzed, concentrated and stored at 4°C.

Antibodies, immunoblotting and RII overlay assays

For western blotting, samples were separated by SDS–PAGE (Bio-Rad pre-cast gels; 4–15% acrylamide gradient) and electrotransferred to nitrocellulose membrane filters (Schleicher & Schuell). Antibody binding was detected by enhanced chemiluminescence (ECL; Pierce). Antibodies used in this study are as follows: Abl (Pharmingen, 8E9; and SantaCruz, K-12), PKA catalytic subunit (Transduction Laboratories), FLAG (Sigma, M2 and M5), GFP (Clontech, Living colors polyclonal antibody), His tag (Amersham Pharmacia Biotech), actin (SantaCruz, C-2), GST (SantaCruz), paxillin (Transduction Laboratories) and RIIα/RIIβ (Upstate Biotechnology Transduction Laboratories). [^{32}P]RII overlay assays were performed as described previously (Carr and Scott, 1992).

Immunoprecipitation

Cell and tissue extracts were prepared as described above and subjected to immunoprecipitation overnight using 10 µg of affinity-purified WAVE antibodies and 25 µl of protein A-conjugated agarose beads (Upstate Biotechnology) or 35 µl of the M2 anti-FLAG monoclonal antibody (Sigma) immobilized on Sepharose beads. The beads were then washed once with 1 ml of lysis buffer, three times with 1 ml of lysis buffer containing 1 M NaCl, and once with 1 ml of lysis buffer. Bound proteins were eluted with Laemmli sample buffer, and subjected to immunoblotting as described above.

PKA assay

Immunoprecipitated FLAG-WAVE-1 from HEK-293 cells or non-transfected control cells was incubated with 10 mM cAMP. PKA activity was measured with the substrate Kemptide as described in the presence or absence of the PKA-specific inhibitor PKI (Corbin and Reimann, 1974).

Immunocytochemistry

Swiss 3T3 fibroblasts were plated on glass coverslips in 6-well plates at 2×10^5 cells per well. After 24 h, cells were washed with serum-free Dulbecco's modified Eagle's medium (DMEM) and serum starved overnight. Cells were then treated for 10 min with 10 ng/ml PDGF (BB homodimer; Upstate Biotechnology), washed with PBS, fixed with 3.7% formaldehyde/PBS for 10 min and permeabilized with 0.5% Triton X-100/PBS for 5 min. After blocking overnight in 1% bovine serum albumin (BSA)/PBS, either specific primary antibodies or non-immune controls were applied in blocking buffer for 1 h at room temperature. Cells were washed, incubated with fluorochrome-conjugated secondary antibodies and Texas red–phalloidin for 1 h, and washed. Cells treated with cytochalasin D (Sigma) were treated for 30 min with 10 μM cytochalasin D prior to treatment with PDGF. Coverslips were mounted using Prolong Antifade reagent (Molecular Probes) and visualized on a Bio-Rad 1024UV laser-scanning confocal microscope equipped with an Axiovert-100 (Zeiss).

Acknowledgements

The authors wish to thank Tony Pawson for the generous gift of GST–SH3 domain expression constructs, Anne Westphal, Robert Mouton and Kimberly Sandstrom for excellent technical assistance, and our colleagues in the Vollum Institute for critical evaluation of the manuscript. This work was supported in part by DK 44239 to J.D.S.

References

Ahern-Djamali,S.M., Bachmann,C., Hua,P., Reddy,S.K., Kastenmeier,A.S., Walter,U. and Hoffmann,F.M. (1999) Identification of profilin and src homology 3 domains as binding partners for *Drosophila* enabled. *Proc. Natl Acad. Sci. USA*, **96**, 4977–4982.

Banin,S., Gout,I. and Brickell,P. (1999) Interaction between Wiskott–Aldrich syndrome protein (WASP) and the Fyn protein-tyrosine kinase. *Mol. Biol. Rep.*, **26**, 173–177.

Bear,J.E., Rawls,J.F. and Saxe,C.L.,III (1998) SCAR, a WASP-related protein, isolated as a suppressor of receptor defects in late *Dictyostelium* development. *J. Cell Biol.*, **142**, 1325–1335.

Blanchoin,L., Amann,K., Higgs,H., Marchland,J.B., Kaiser,D. and Pollard,T. (2000) Direct observation of dendritic actin filament networks nucleated by Arp2/3 complex and WASP/Scar proteins. *Nature*, **404**, 1007–1011.

Bunnell,S.C., Henry,P.A., Kolluri,R., Kirchhausen,T., Rickles,R.J. and Berg,L.J. (1996) Identification of Itk/Tsk Src homology 3 domain ligands. *J. Biol. Chem.*, **271**, 25646–25656.

Carlier,M.F. *et al*. (2000) GRB2 links signalling to actin assembly by enhancing interaction of neural Wiskott–Aldrich syndrome protein (N-Wasp) with actin-related-protein (ARP2/3) complex. *J. Biol. Chem.*, **275**, 21946–21952.

Carr,D.W. and Scott,J.D. (1992) Blotting and band-shifting: techniques for studying protein–protein interactions. *Trends Biochem. Sci.*, **17**, 246–249.

Carr,D.W., Stofko-Hahn,R.E., Fraser,I.D.C., Bishop,S.M., Acott,T.S., Brennan,R.G. and Scott,J.D. (1991) Interaction of the regulatory subunit (RII) of cAMP-dependent protein kinase with RII-anchoring proteins occurs through an amphipathic helix binding motif. *J. Biol. Chem.*, **266**, 14188–14192.

Carr,D.W., Hausken,Z.E., Fraser,I.D.C., Stofko-Hahn,R.E. and Scott,J.D. (1992) Association of the type II cAMP-dependent protein kinase with a human thyroid RII-anchoring protein, cloning and characterization of the RII-binding domain. *J. Biol. Chem.*, **267**, 13376–13382.

Colledge,M. and Scott,J.D. (1999) AKAPs: from structure to function. *Trends Cell Biol.*, **9**, 216–221.

Corbin,J.D. and Reimann,E.M. (1974) A filter assay for determining protein kinase activity. *Methods Enzymol.*, **38**, 287–294.

Cory,G.O., MacCarthy-Morrogh,L., Banin,S., Gout,I., Brickell,P.M., Levinsky,R.J., Kinnon,C. and Lovering,R.C. (1996) Evidence that the Wiskott–Aldrich syndrome protein may be involved in lymphoid cell signaling pathways. *J. Immunol.*, **157**, 3791–3795.

Finan,P.M., Soames,C.J., Wilson,L., Nelson,D.L., Stewart,D.M., Truong,O., Hsuan,J.J. and Kellie,S. (1996) Identification of regions of the Wiskott–Aldrich syndrome protein responsible for association with selected Src homology 3 domains. *J. Biol. Chem.*, **271**, 26291–26295.

Gertler,F.B., Hill,K.K., Clark,M.J. and Hoffmann,F.M. (1993) Dosage-sensitive modifiers of *Drosophila* abl tyrosine kinase function: prospero, a regulator of axonal outgrowth and disabled, a novel tyrosine kinase substrate [published erratum appears in *Genes Dev.*, 1996, **10**, 2234]. *Genes Dev.*, **7**, 441–453.

Gertler,F.B., Comer,A.R., Juang,J.L., Ahern,S.M., Clark,M.J., Liebl,E.C. and Hoffmann,F.M. (1995) *enabled*, a dosage-sensitive suppressor of mutations in the *Drosophila* Abl tyrosine kinase, encodes an Abl substrate with SH3 domain-binding properties. *Genes Dev.*, **9**, 521–533.

Hall,A. (1998) Rho GTPases and the actin cytoskeleton. *Science*, **279**, 509–514.

Hausken,Z.E., Dell'Acqua,M.L., Coghlan,V.M. and Scott,J.D. (1996) Mutational analysis of the A-kinase anchoring protein (AKAP)-binding site on RII. *J. Biol. Chem.*, **271**, 29016–29022.

Hausken,Z.E., Coghlan,V.M. and Scott,J.D. (1998) Overlay, ligand blotting and band-shift techniques to study kinase anchoring. In Clegg,R.A. (ed.), *Protein Targeting Protocols*, Vol. 88. Humana Press, Totowa, NJ, pp. 47–64.

Herberg,F.W., Maleszka,A., Eide,T., Vossebein,L. and Tasken,K. (2000) Analysis of A-kinase anchoring protein (AKAP) interaction with protein kinase A (PKA) regulatory subunits: PKA isoform specificity in AKAP binding. *J. Mol. Biol.*, **298**, 329–339.

Higgs,H.N. and Pollard,T.D. (1999) Regulation of actin polymerization by Arp2/3 complex and WASp/Scar proteins. *J. Biol. Chem.*, **274**, 32531–32534.

Kim,A.S., Kakalis,L.T., Abdul-Manan,N., Liu,G.A. and Rosen,M.K. (2000) Autoinhibition and activation mechanisms of the Wiskott–Aldrich syndrome protein. *Nature*, **404**, 151–158.

Kinnon,C., Cory,G.O., MacCarthy-Morrogh,L., Banin,S., Gout,I., Lovering,R.C. and Brickell,P.M. (1997) The identification of Bruton's tyrosine kinase and Wiskott–Aldrich syndrome protein associated proteins and signalling pathways. *Biochem. Soc. Trans.*, **25**, 648–650.

Lewis,J.M. and Schwartz,M.A. (1998) Integrins regulate the association and phosphorylation of paxillin by c-Abl. *J. Biol. Chem.*, **273**, 14225–14230.

Machesky,L.M. and Insall,R.H. (1998) Scar1 and the related Wiskott–Aldrich syndrome protein, WASP, regulate the actin cytoskeleton through the Arp2/3 complex. *Curr. Biol.*, **8**, 1347–1356.

Machesky,L.M., Mullins,R.D., Higgs,H.N., Kaiser,D.A., Blanchoin,L., May,R.C., Hall,M.E. and Pollard,T.D. (1999) Scar, a WASp-related protein, activates nucleation of actin filaments by the Arp2/3 complex. *Proc. Natl Acad. Sci. USA*, **96**, 3739–3744.

McWhirter,J.R. and Wang,J.Y. (1991) Activation of tyrosinase kinase and microfilament-binding functions of c-abl by bcr sequences in bcr/abl fusion proteins. *Mol. Cell. Biol.*, **11**, 1553–1565.

Miki,H., Miura,K. and Takenawa,T. (1996) N-WASP, a novel actin-depolymerizing protein, regulates the cortical cytoskeletal rearrangement in a PIP2-dependent manner downstream of tyrosine kinases. *EMBO J.*, **15**, 5326–5335.

Miki,H., Suetsugu,S. and Takenawa,T. (1998) WAVE, a novel WASP-family protein involved in actin reorganization induced by Rac. *EMBO J.*, **17**, 6932–6941.

Ming,G.L., Song,H.J., Berninger,B., Holt,C.E., Tessier-Lavigne,M. and Poo,M.M. (1997) cAMP-dependent growth cone guidance by netrin-1. *Neuron*, **19**, 1225–1235.

Mullins,R.D. (2000) How WASP-family proteins and the Arp2/3 complex convert intracellular signals into cytoskeletal structures. *Curr. Opin. Cell Biol.*, **12**, 91–96.

Nagase,T. *et al*. (1996) Prediction of the coding sequences of unidentified human genes. VI. The coding sequences of 80 new genes (KIAA0201–KIAA0280) deduced by analysis of cDNA clones from cell line KG-1 and brain. *DNA Res.*, **3**, 321–329, 341–354.

Newlon,M.G., Roy,M., Morikis,D., Hausken,Z.E., Coghlan,V., Scott,J.D. and Jennings,P.A. (1999) The molecular basis for protein kinase A anchoring revealed by solution NMR. *Nature Struct. Biol.*, **6**, 222–227.

Nobes,C.D., Hawkins,P., Stephens,L. and Hall,A. (1995) Activation of the small GTP-binding proteins rho and rac by growth factor receptors. *J. Cell Sci.*, **108**, 225–233.

Pawson,T. and Gish,G.D. (1992) SH2 and SH3 domains: from structure to function. *Cell*, **71**, 359–362.

Pawson,T. and Scott,J.D. (1997) Signaling through scaffold, anchoring and adaptor proteins. *Science*, **278**, 2075–2080.

Pendergast,A.M. (1996) Nuclear tyrosine kinases: from Abl to WEE1. *Curr. Opin. Cell Biol.*, **8**, 174–181.

Scott,J.D., Fischer,E.H. and Krebs,E.G. (1985) The inhibitory region of the heat-stable protein inhibitor of the cAMP-dependent protein kinase. *FASEB J.*, **2**, 703.

Snapper,S.B. and Rosen,F.S. (1999) The Wiskott–Aldrich syndrome protein (WASP): roles in signaling and cytoskeletal organization. *Annu. Rev. Immunol.*, **17**, 905–929.

Song,H.J., Ming,G.L. and Poo,M.M. (1997) cAMP-induced switching in turning direction of nerve growth cones [published erratum appears in *Nature*, 1997, **389**, 412]. *Nature*, **388**, 275–279.

Sparks,A.B., Rider,J.E., Hoffman,N.G., Fowlkes,D.M., Quillam,L.A. and Kay,B.K. (1996) Distinct ligand preferences of Src homology 3 domains from Src, Yes, Abl, cortactin, p53bp2, PLCγ, Crk and Grb2. *Proc. Natl Acad. Sci. USA*, **93**, 1540–1544.

Suetsugu,S., Miki,H. and Takenawa,T. (1999) Identification of two human WAVE/SCAR homologues as general actin regulatory molecules which associate with the Arp2/3 complex. *Biochem. Biophys. Res. Commun.*, **260**, 296–302.

Vaduva,G., Martin,N.C. and Hopper,A.K. (1997) Actin-binding verprolin is a polarity development protein required for the morphogenesis and function of the yeast actin cytoskeleton. *J. Cell Biol.*, **139**, 1821–1833.

Wills,Z., Bateman,J., Korey,C.A., Comer,A. and Van Vactor,D. (1999) The tyrosine kinase Abl and its substrate enabled collaborate with the receptor phosphatase Dlar to control motor axon guidance. *Neuron*, **22**, 301–312.

Received May 16, 2000; revised June 9, 2000;
accepted July 5, 2000